

**ORIGINAL CONTAINS  
COLOR ILLUSTRATIONS**

WASHINGTON UNIVERSITY  
DEPARTMENT OF PHYSICS  
LABORATORY FOR ULTRASONICS  
St. Louis, Missouri 63130

100-100  
10-33-CR  
SCIT.  
49945  
12-16

**"Physical Interpretation and Development of Ultrasonic Nondestructive  
Evaluation Techniques Applied to the Quantitative Characterization of Textile  
Composite Materials"**

Semiannual Progress Report: September 15, 1994 - March 14, 1995

NASA Grant Number: NSG-1601

Principal Investigator:

Dr. James G. Miller  
Professor of Physics

The NASA Technical Officer for this grant is:

Dr. Patrick H. Johnston  
NASA Langley Research Center  
Hampton, Virginia

N95-28034

Unclass

0049945

G3/38

(NASA-CR-198591) PHYSICAL  
INTERPRETATION AND DEVELOPMENT OF  
ULTRASONIC NONDESTRUCTIVE  
EVALUATION TECHNIQUES APPLIED TO  
THE QUANTITATIVE CHARACTERIZATION  
OF TEXTILE COMPOSITE MATERIALS  
Semiannual Progress Report, 15 Sep.  
1994 - 14 Mar. 1995 (Washington  
Univ.) 16 p

## **I. Introduction**

In this Progress Report, we describe our continuing research to explore the feasibility of implementing medical linear array imaging technology as a viable ultrasonic-based nondestructive evaluation method to inspect and characterize complex materials. We present images obtained using an unmodified medical ultrasonic imaging system of a bonded aluminum plate sample with a simulated disbond region. The disbond region was produced by adhering a piece of plain white paper to a piece of cellophane tape and applying the paper-tape combination to one of the aluminum plates. Because the area under the paper was not adhesively bonded to the aluminum plate we feel that this arrangement more closely simulates a disbond. Images are also presented for an aluminum plate sample with an epoxy strip adhered to one side to help provide information for the interpretation of the images of the bonded aluminum plate sample containing the disbond region. These images are compared with corresponding conventional ultrasonic contact transducer measurements in order to provide information regarding the nature of the disbonded region. We anticipate the results of this on-going investigation may provide a step toward the development of a rapid, real-time, and portable method of ultrasonic inspection and characterization based on linear array technology.

In the Section II of this Progress Report we describe the preparation of the aluminum plate specimens interrogated. Section III describes the method of linear array imaging. Sections IV and V present the linear array images and results from contact transducer measurements, respectively. A discussion of the results are presented in Section VI.

## **II. Sample Preparation**

Two aluminum/epoxy samples were prepared for the investigation. One sample consisted of two aluminum plates bonded with epoxy which contained a region of simulated disbond. The other sample was a single plate of aluminum with a strip of epoxy adhered to one side.

### ***Bonded Aluminum Plate Sample (Sample F)***

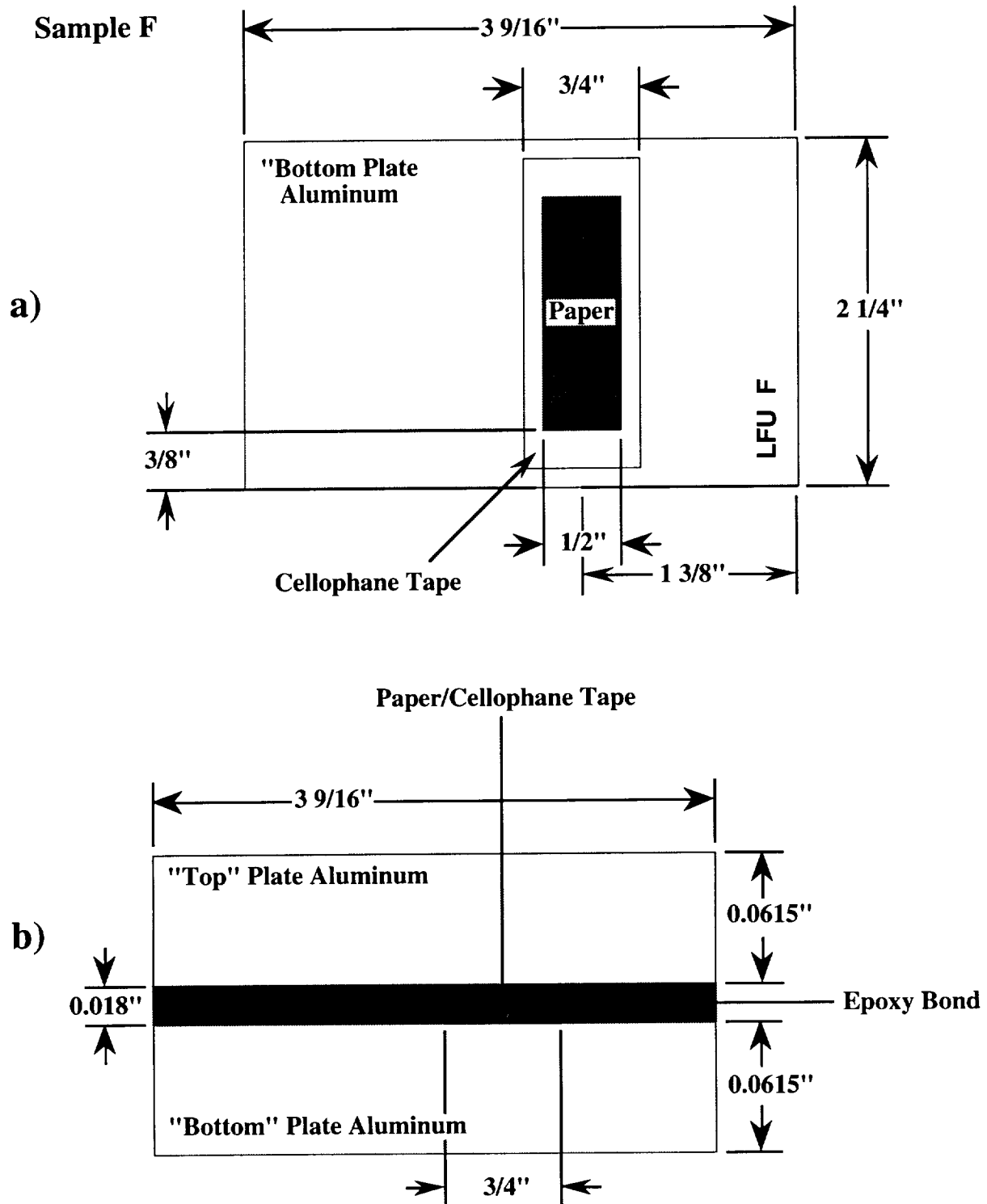
The bonded aluminum plate sample (sample F) interrogated in this investigation was 2 1/4" wide by 3 9/16" in length. Two identical aluminum plates of 0.0615" in thickness were used in the production of sample F. The sample was constructed with an area of layered paper/cellophane tape to simulate a disbanded region. The bonded plate sample was produced by adhering a piece of plain white paper (0.0038" thick, 1/2" wide by 1 1/2" long) to a piece of cellophane tape (3/4" wide by 1 1/2" long). The paper-tape was applied to the "bottom" plate. "Duro Master Mend™" epoxy was applied to the "bottom" plate which had the paper/cellophane tape attached and a "top" aluminum plate was applied. Weights were applied to the sample to produce a constant compressive force during the cure process. After the epoxy had cured the specimens were machined to their final length and width dimensions leaving only one area of simulated disbond. The final thickness of sample F was 0.141". Figure 1 illustrates how sample F was constructed.

### ***Single Plate of Aluminum With an Epoxy Strip (Sample E)***

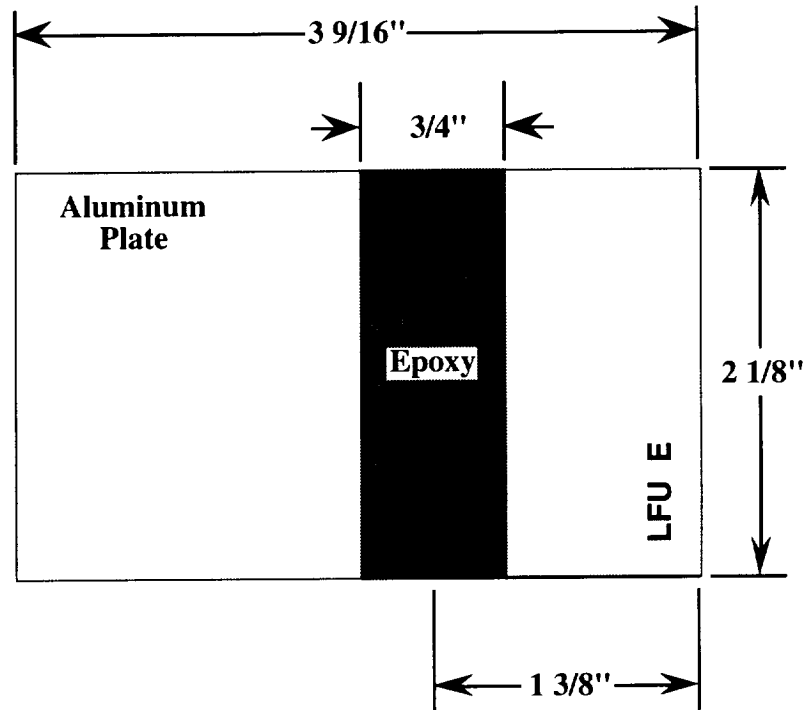
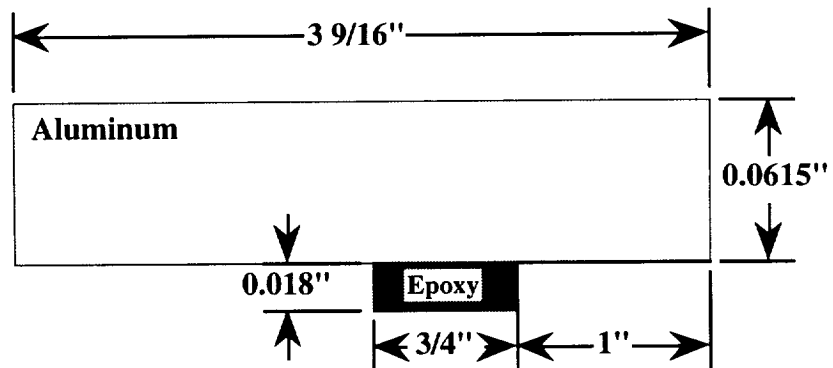
In order to compare the effects on the reflected ultrasound at the aluminum/paper interface ("disbond") to the well-bonded regions of sample F, a single plate aluminum sample (sample E) was constructed with a strip of epoxy applied to one side. The aluminum plate was 3 9/16" in length by 2 1/8" wide and 0.0615" thick and the epoxy strip was 3/4" wide by 2 1/8" long. The measured total thickness of the resultant aluminum plus epoxy region was 0.0729". Figure 2 illustrates the construction of the aluminum/epoxy-strip sample.

## **III. Method of Linear Array Imaging**

The aluminum plate samples were imaged with an unmodified Hewlett-Packard SONOS 1500 medical imaging system in the peripheral vascular imaging mode. A nominal 7.5 MHz center-frequency linear array probe was used with an overall length of 1.5 inches. Between the sample and the linear array probe a gelatin stand-off was employed as illustrated in Figure 3. The gelatin stand-off served to move the front surface echo of the aluminum specimens closer to the center of



**Figure 1:** Illustration of the construction of the sample F (the bonded aluminum plate sample). a) Looking down on the "bottom" plate b) A cross-sectional representation, the horizontal dimension is to scale while the vertical dimension is exaggerated (x 3.4) for clarity.

**Sample E****a)****b)**

**Figure 2:** Illustration of the construction of the sample E (the aluminum plate with epoxy sample). a) Looking down on the aluminum plate b) A cross-sectional representation, the horizontal dimension is to scale while the vertical dimension is exaggerated (x 3.4) for clarity.

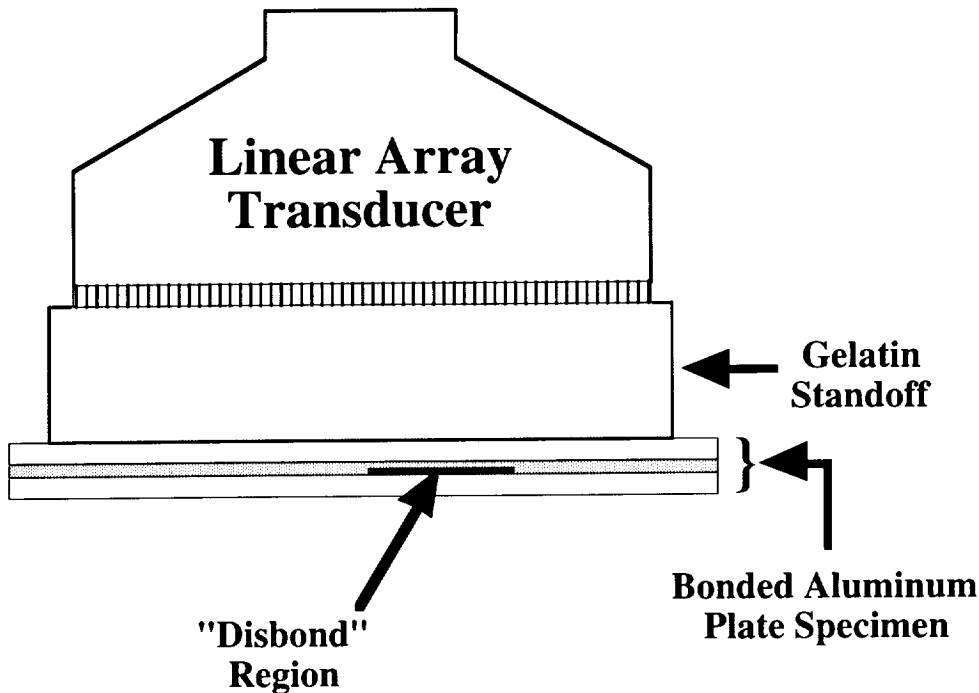


**Figure 3:** Configuration of linear array transducer and gelatin standoff for obtaining images of the samples.

the image. Each sample was imaged with the axis of the linear array along the long axis (length dimension) of the sample so that the linear array straddled the disbond region. The transmit power level of the SONOS 1500 imaging system was kept constant and the same depth dependent gain (time-gain compensation) was applied to all depth segments for all the measurements. For each sample interrogated the video compression was adjusted to optimize the image contrast and remained constant.

The disbonded region and surrounding regions of sample F were imaged from both sides of the specimen; i.e., sample F was imaged from the aluminum plate side in contact with the paper-cellophane tape ("bottom" side) as well as on the opposite side ("top" side). Sample E was interrogated from the aluminum plate side of the sample.

Figure 4 illustrates how to interpret the images presented of the samples obtained with the linear array system. For sample F the images were acquired with the linear array straddling the

disbond region (imaged from the "top" plate side and the "bottom" plate side). For sample E, the aluminum plate plus the epoxy strip sample, the linear array insonified from the aluminum plate side of the sample straddling the epoxy strip. As discussed in the September 1994 Progress Report these images are composed of many reverberations of the ultrasonic signal in the sample and do not represent a single cross-sectional view. The general pattern seen in the images (as depicted in Figure 4) will be lightly shaded regions on either side of the disbond region for sample F and the epoxy strip region for sample E. The center portion of the image will display a characteristic reverberation pattern dependent on the type of interfaces encountered for the given sample. In the areas of the image representing the disbond region of sample F the exact shading of the reverberating signal will depend on the side of insonification.

#### **IV. Linear Array Images**

Figure 5 shows the linear array B-scan image over the epoxy region for the sample with the epoxy strip (sample E). The image was acquired by insonifying the aluminum plate side of the sample (opposite to the side with the epoxy strip). The strip of epoxy region is clearly distinguished from the aluminum plate only regions. The side regions which represent the aluminum/air interface display a reverberation decay pattern that appears bright and long in duration. This is to be expected because the aluminum to air interface presents a large acoustic impedance mismatch and a large portion of the acoustic energy is reflected at this interface. Because aluminum is a rather low-loss material, we see a bright and long decay pattern. The center portion of the image displays the area of the aluminum/epoxy interface. A smaller acoustic impedance mismatch is presented to the acoustic wave in this region and thus some acoustic energy travels into the epoxy region. Because epoxy is more attenuating than aluminum we see that the reverberation pattern appears to be less bright and shorter in duration than the surrounding side regions.

## Cartoon Depicting Typical Linear Array Images

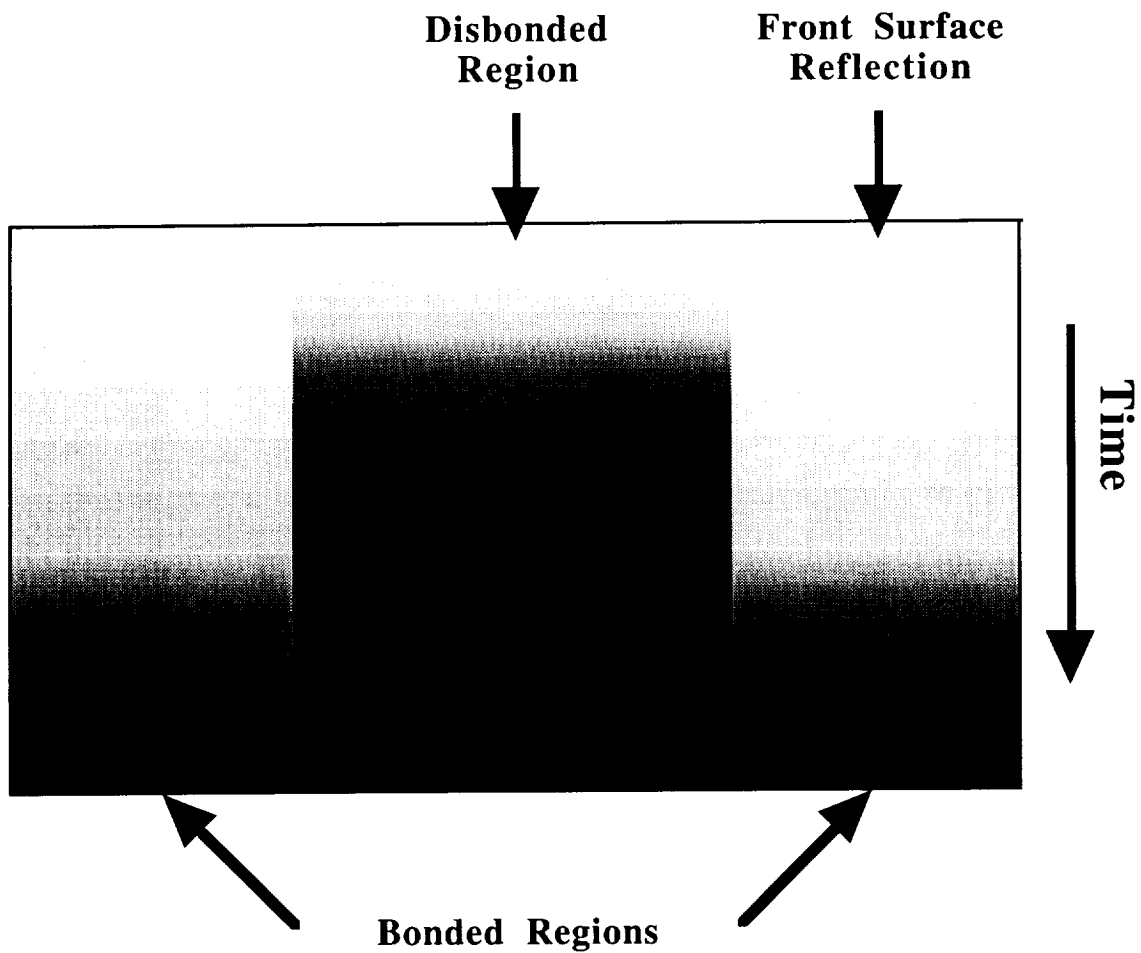


**Figure 4:** Cartoon showing how to interpret the linear array images.



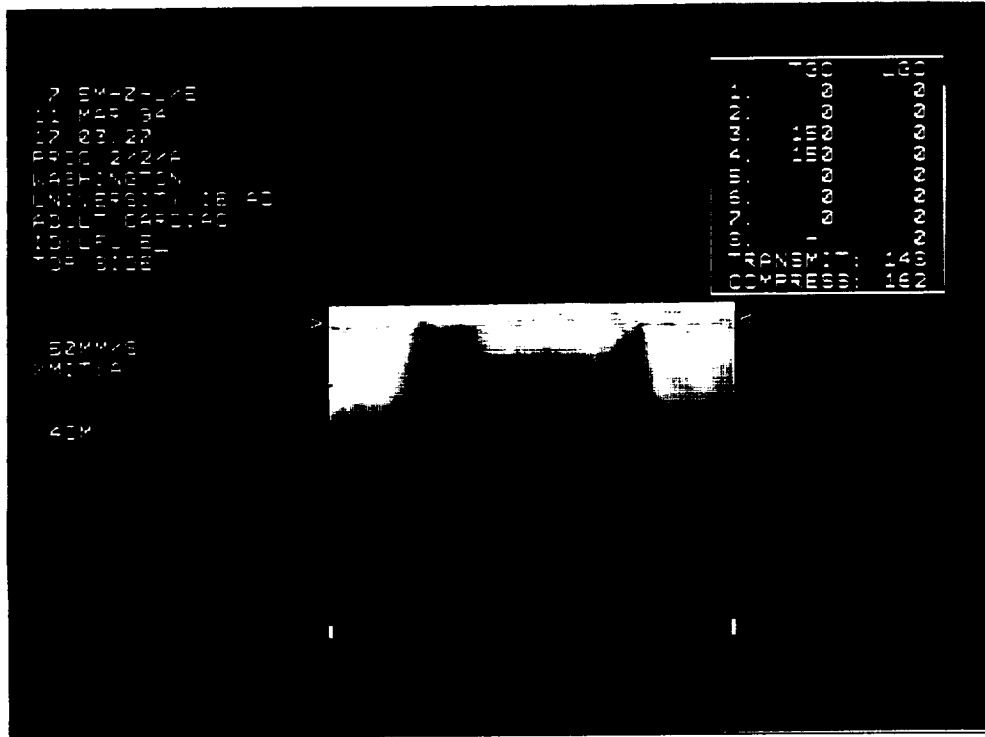


**Figure 5 - Linear array image over the epoxy strip region of sample E.**

Figure 6 shows the linear array B-scan images over the disbonded region for sample F from both sides. In Figure 6a the image was acquired by insonifying the "bottom" side of the sample where the paper-tape was adhered to the aluminum plate. The region of the disbond can be clearly distinguished from the surrounding well-bonded region in this image. The aluminum/paper interface appears to present a greater acoustic impedance mismatch than the aluminum/epoxy regions on either side of the disbond region. Since epoxy is considerably more attenuating than aluminum, more acoustic energy is reflected at the aluminum/paper interface than at the aluminum/epoxy interface and we see a brighter and longer decay pattern. This decay pattern results from the reverberation of the acoustic energy in the "bottom" aluminum plate.

Figure 6b shows the B-scan image of the disbonded region of sample F obtained from the "top" side of the specimen. In this image the region of disbond can again be clearly distinguished

from the surrounding well-bonded region although it appears different than that observed when imaged from the "bottom" side of the sample (Figure 6a). If we compare the center portion of the image of Figure 6b with the center portion of Figure 5, we see that the decay patterns display similar features. This is the same situation encountered when imaging the epoxy strip sample in sample E. Ultrasound propagates through the "top" aluminum plate and into the epoxy before encountering the air interface. Hence, the echo decay pattern observed for the sample over the disbond when imaged from the "top" side is similar to the image of the epoxy strip in sample E. This acoustic impedance mismatch reflects a large portion of the acoustic energy. The resultant decay pattern is dominated by the reverberation in the "top" aluminum plate and the epoxy layer. Because epoxy is more attenuating than aluminum the epoxy layer dampens the decay pattern. The well-bonded side regions (aluminum/epoxy/aluminum regions) appear to be very similar in the two images. We would expect the images from the well-bonded regions to be very similar when imaged from both sides of the sample because the thickness of each of the aluminum plates is the same and hence the ultrasound propagates along the same path in both cases.

## **V. Contact Transducer Measurements**

In order to substantiate the interpretations of the images of the aluminum plate specimens obtained with the linear array, single element contact transducer measurements were performed. Ultrasonic rf A-lines from the bonded and disbonded regions of sample F were obtained from each side of the specimen. For sample E the side opposite the epoxy strip was insonified. The rf A-lines from sample E were obtained from both the aluminum only area and the aluminum/epoxy area of the sample. Pulse-echo measurements were made with a broadband, 1/4" diameter, 25 MHz contact transducer (KB Aerotech - Alpha DFR) with a 3/8" delay line. A Metrotek MP215 pulser was used to generate the broadband excitation pulse and a MR106 receiver was employed to amplify the returned ultrasonic signal. The returned rf signal was taken from the MR106 receiver output and sent to a Tektronix TDS 520 digitizing oscilloscope. Signals were digitized at a rate of

1. 2. 3. 4. 5. 6. 7. 8. 9. 10. 11. 12. 13. 14. 15. 16. 17. 18. 19. 20. 21. 22. 23. 24. 25. 26. 27. 28. 29. 30. 31. 32. 33. 34. 35. 36. 37. 38. 39. 40. 41. 42. 43. 44. 45. 46. 47. 48. 49. 50. 51. 52. 53. 54. 55. 56. 57. 58. 59. 60. 61. 62. 63. 64. 65. 66. 67. 68. 69. 70. 71. 72. 73. 74. 75. 76. 77. 78. 79. 80. 81. 82. 83. 84. 85. 86. 87. 88. 89. 90. 91. 92. 93. 94. 95. 96. 97. 98. 99. 100. 101. 102. 103. 104. 105. 106. 107. 108. 109. 110. 111. 112. 113. 114. 115. 116. 117. 118. 119. 120. 121. 122. 123. 124. 125. 126. 127. 128. 129. 130. 131. 132. 133. 134. 135. 136. 137. 138. 139. 140. 141. 142. 143. 144. 145. 146. 147. 148. 149. 150. 151. 152. 153. 154. 155. 156. 157. 158. 159. 160. 161. 162. 163. 164. 165. 166. 167. 168. 169. 170. 171. 172. 173. 174. 175. 176. 177. 178. 179. 180. 181. 182. 183. 184. 185. 186. 187. 188. 189. 190. 191. 192. 193. 194. 195. 196. 197. 198. 199. 200. 201. 202. 203. 204. 205. 206. 207. 208. 209. 210. 211. 212. 213. 214. 215. 216. 217. 218. 219. 220. 221. 222. 223. 224. 225. 226. 227. 228. 229. 230. 231. 232. 233. 234. 235. 236. 237. 238. 239. 240. 241. 242. 243. 244. 245. 246. 247. 248. 249. 250. 251. 252. 253. 254. 255. 256. 257. 258. 259. 260. 261. 262. 263. 264. 265. 266. 267. 268. 269. 270. 271. 272. 273. 274. 275. 276. 277. 278. 279. 280. 281. 282. 283. 284. 285. 286. 287. 288. 289. 290. 291. 292. 293. 294. 295. 296. 297. 298. 299. 300. 301. 302. 303. 304. 305. 306. 307. 308. 309. 310. 311. 312. 313. 314. 315. 316. 317. 318. 319. 320. 321. 322. 323. 324. 325. 326. 327. 328. 329. 330. 331. 332. 333. 334. 335. 336. 337. 338. 339. 340. 341. 342. 343. 344. 345. 346. 347. 348. 349. 350. 351. 352. 353. 354. 355. 356. 357. 358. 359. 360. 361. 362. 363. 364. 365. 366. 367. 368. 369. 370. 371. 372. 373. 374. 375. 376. 377. 378. 379. 380. 381. 382. 383. 384. 385. 386. 387. 388. 389. 390. 391. 392. 393. 394. 395. 396. 397. 398. 399. 400. 401. 402. 403. 404. 405. 406. 407. 408. 409. 410. 411. 412. 413. 414. 415. 416. 417. 418. 419. 420. 421. 422. 423. 424. 425. 426. 427. 428. 429. 430. 431. 432. 433. 434. 435. 436. 437. 438. 439. 440. 441. 442. 443. 444. 445. 446. 447. 448. 449. 450. 451. 452. 453. 454. 455. 456. 457. 458. 459. 460. 461. 462. 463. 464. 465. 466. 467. 468. 469. 470. 471. 472. 473. 474. 475. 476. 477. 478. 479. 480. 481. 482. 483. 484. 485. 486. 487. 488. 489. 490. 491. 492. 493. 494. 495. 496. 497. 498. 499. 500. 501. 502. 503. 504. 505. 506. 507. 508. 509. 510. 511. 512. 513. 514. 515. 516. 517. 518. 519. 520. 521. 522. 523. 524. 525. 526. 527. 528. 529. 530. 531. 532. 533. 534. 535. 536. 537. 538. 539. 540. 541. 542. 543. 544. 545. 546. 547. 548. 549. 550. 551. 552. 553. 554. 555. 556. 557. 558. 559. 560. 561. 562. 563. 564. 565. 566. 567. 568. 569. 570. 571. 572. 573. 574. 575. 576. 577. 578. 579. 580. 581. 582. 583. 584. 585. 586. 587. 588. 589. 590. 591. 592. 593. 594. 595. 596. 597. 598. 599. 600. 601. 602. 603. 604. 605. 606. 607. 608. 609. 610. 611. 612. 613. 614. 615. 616. 617. 618. 619. 620. 621. 622. 623. 624. 625. 626. 627. 628. 629. 630. 631. 632. 633. 634. 635. 636. 637. 638. 639. 640. 641. 642. 643. 644. 645. 646. 647. 648. 649. 650. 651. 652. 653. 654. 655. 656. 657. 658. 659. 660. 661. 662. 663. 664. 665. 666. 667. 668. 669. 670. 671. 672. 673. 674. 675. 676. 677. 678. 679. 680. 681. 682. 683. 684. 685. 686. 687. 688. 689. 690. 691. 692. 693. 694. 695. 696. 697. 698. 699. 700. 701. 702. 703. 704. 705. 706. 707. 708. 709. 710. 711. 712. 713. 714. 715. 716. 717. 718. 719. 720. 721. 722. 723. 724. 725. 726. 727. 728. 729. 730. 731. 732. 733. 734. 735. 736. 737. 738. 739. 740. 741. 742. 743. 744. 745. 746. 747. 748. 749. 750. 751. 752. 753. 754. 755. 756. 757. 758. 759. 760. 761. 762. 763. 764. 765. 766. 767. 768. 769. 770. 771. 772. 773. 774. 775. 776. 777. 778. 779. 780. 781. 782. 783. 784. 785. 786. 787. 788. 789. 790. 791. 792. 793. 794. 795. 796. 797. 798. 799. 800. 801. 802. 803. 804. 805. 806. 807. 808. 809. 810. 811. 812. 813. 814. 815. 816. 817. 818. 819. 820. 821. 822. 823. 824. 825. 826. 827. 828. 829. 830. 831. 832. 833. 834. 835

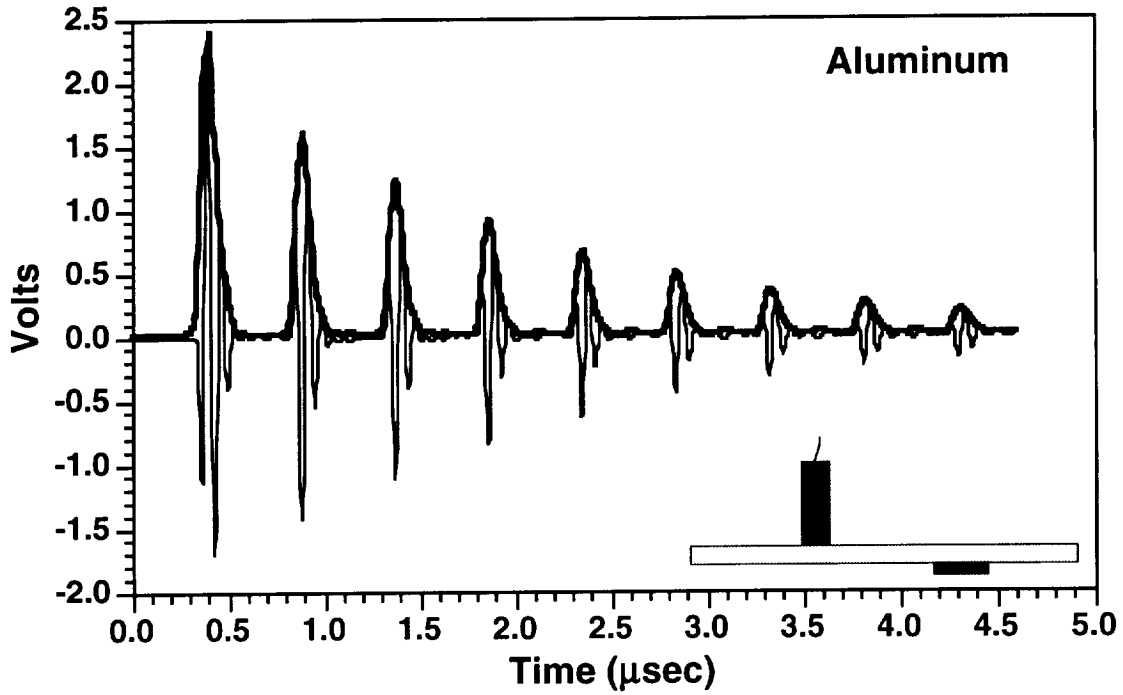
**Figure 6:** Linear array images over the disbanded region for sample F. Figure 6a shows the B-scan image of the disbanded region obtained from the "bottom" side of the specimen. Figure 6b shows the B-scan image of the disbanded region obtained from the "top" side of the specimen.

250 megasamples/second with 8-bit resolution over a total record length of 2500 points. The digitized rf signals were stored on a Macintosh Quadra 840AV for off-line analyses.

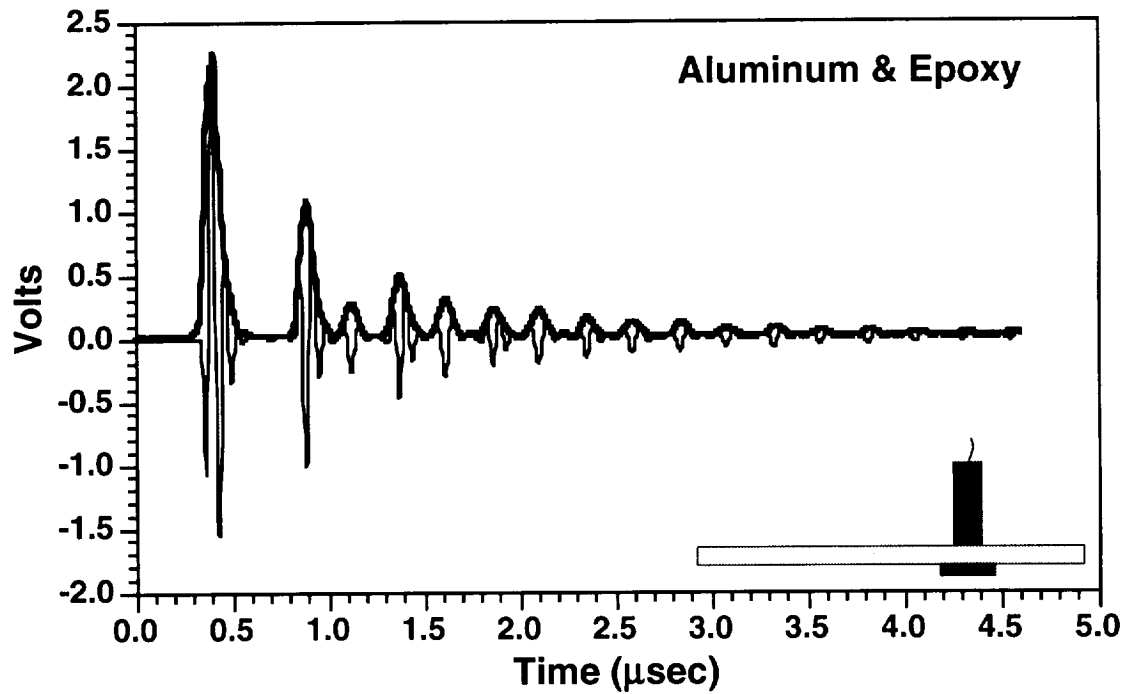
In what follows all the figures displaying the signals obtained with the 25 MHz contact transducer will show both the rf and the magnitude of the analytic signal of the rf superimposed to help guide the eye to the encountered interfaces. Figure 7a displays the rf A-line acquired over the aluminum only portion of sample E. The velocity of sound for aluminum is about 6.35 mm/ $\mu$ sec which for a thickness of 0.0615" yields a round trip time (distance traveled is 2 times 0.0615") between reverberations of 0.492  $\mu$ sec. Figure 7b displays the ultrasonic signals over the aluminum/epoxy region of the sample. We see additional reflections inserted between the aluminum echoes. These reflections occur due to the epoxy to air interface. If we compare Figure 7a and 7b we see that the decay patterns decrease more rapidly for the aluminum/epoxy region than for the aluminum only region. As discussed above, this is what we would expect because the ultrasound that travels into the epoxy region decays more rapidly due to the higher attenuation of the epoxy as compared with aluminum. These reverberation decay patterns are responsible for the resultant decay patterns observed in the linear array image of sample E (see Figure 5).

Figures 8 and 9 display the rf A-lines obtained from the bonded aluminum plate sample (sample F). Figure 8a displays the rf and analytic signal for insonification of the "bottom" side in a well-bonded region of sample F. Figure 8b displays the signals when the sample was flipped over and insonified in the same region as Figure 8a but from the opposite side. We see that the signals in 8a and 8b appear to be quite similar. This is to be expected since the thickness of the two aluminum plates are equal.

In Figure 9a sample F was insonified from the "bottom" side of the specimen (the side to which the paper-tape was applied) with the transducer positioned over the region of the disbond. Figure 9b displays the rf A-line and analytic signal for the same region except that the sample is

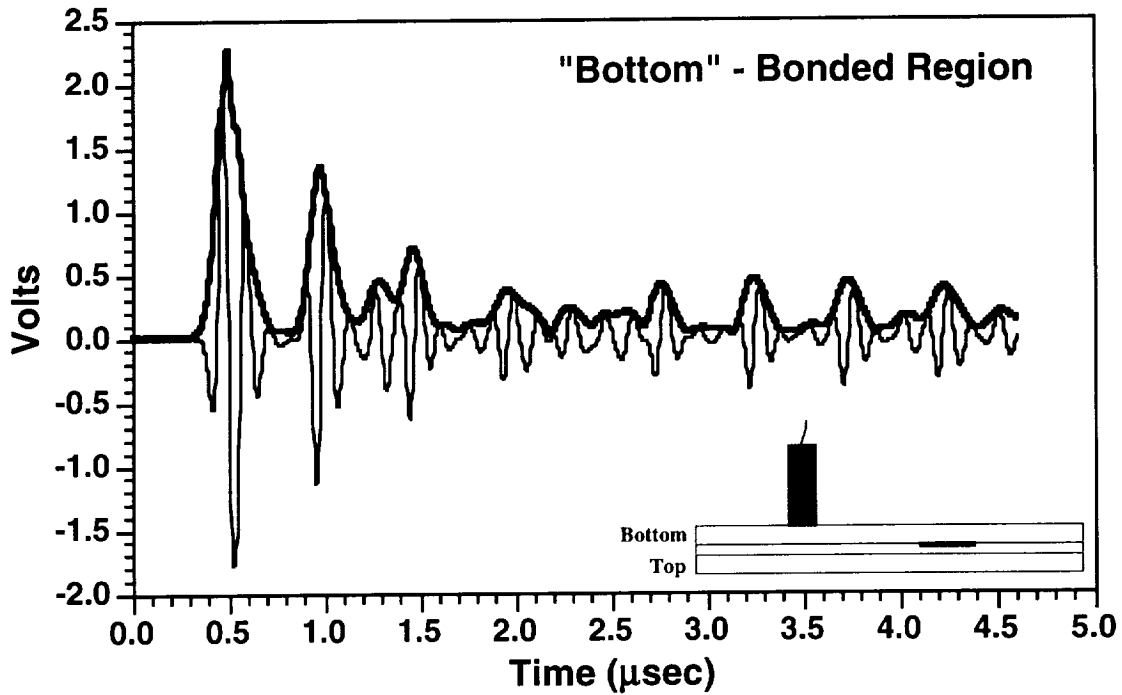


a)

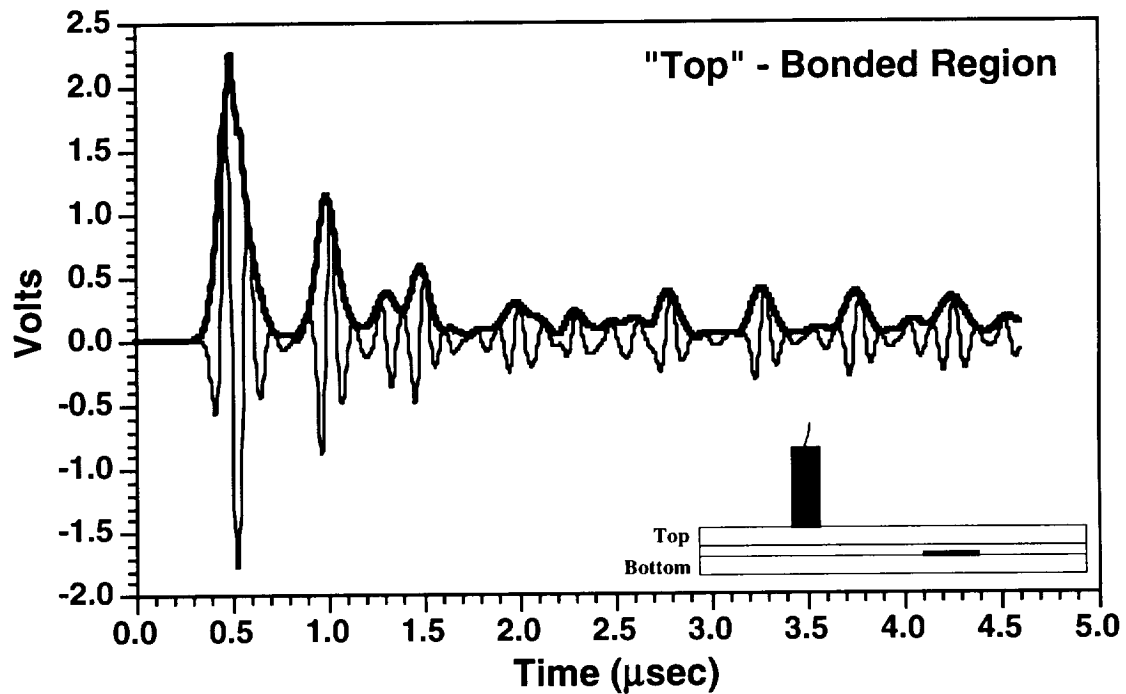


b)

**Figure 7:** The rf and analytic signal of the rf for sample E. a) Insonification of an aluminum only region b) Insonification over the epoxy strip region

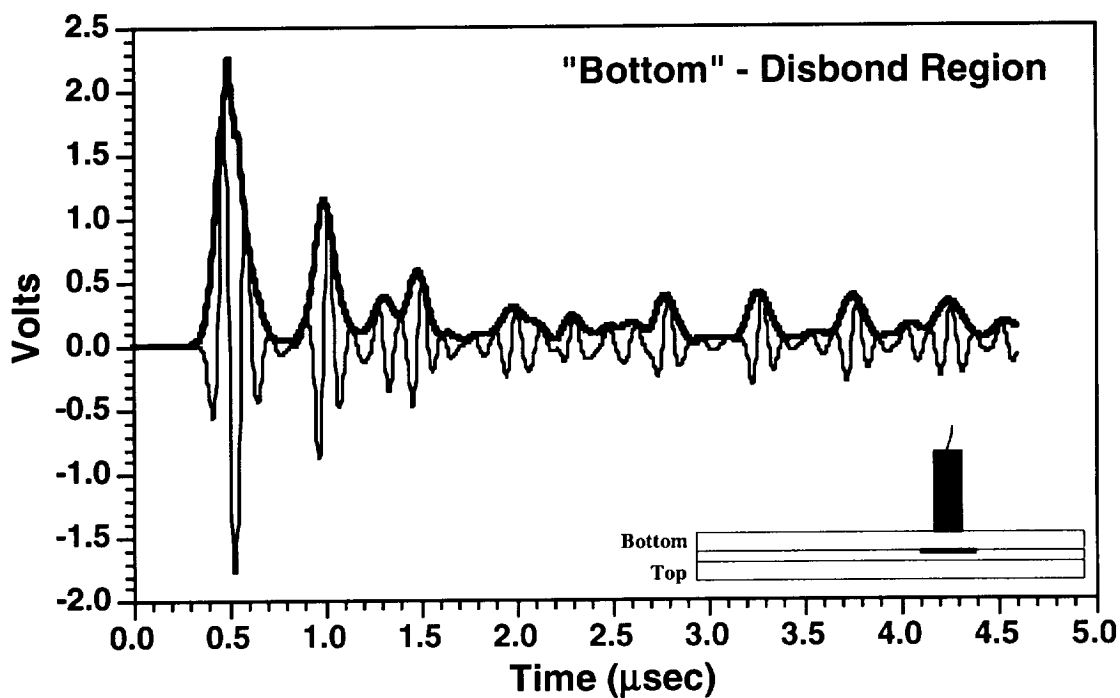


a)

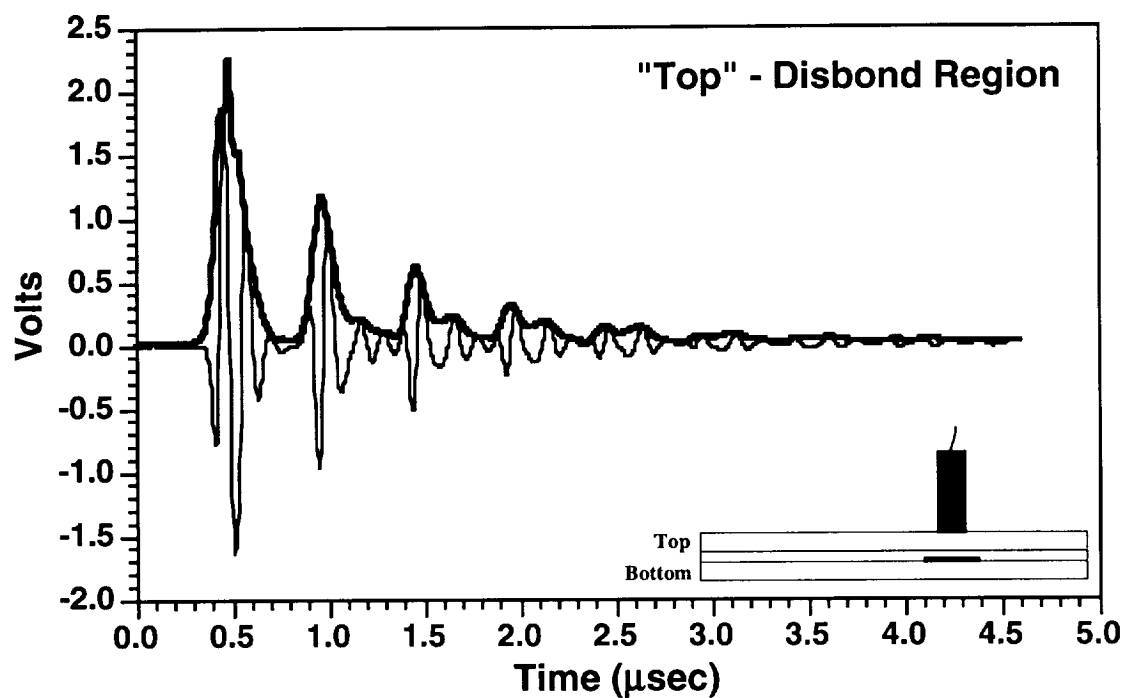


b)

**Figure 8:** The rf and analytic signal of the rf for sample F over the well-bonded area. a) Insonification from the "bottom" side, the side where the paper-tape was adhered b) Insonification from the "top" side



a)



b)

**Figure 9:** The rf and analytic signal of the rf for sample F over the "disbonded" area. a) Insonification from the "bottom" side, the side where the paper-tape was adhered b) Insonification from the "top" side

insonified from the "top" side of the sample. The rf signal for insonification of the "top" side decays more rapidly than the rf obtained from insonifying the "bottom" side. As discussed above because epoxy is more attenuating than aluminum the epoxy layer dampens the decay pattern. If we compare Figure 9a with Figures 8a and 8b we see that they all appear very similar.

## **VI. Discussion**

The results presented above, showing the images of the bonded aluminum plate specimen and the aluminum/epoxy-strip specimen obtained with the linear array and the corresponding ultrasonic rf A-lines obtained with a contact transducer, suggest that linear array imaging can perform a useful role in detecting disbonded regions and providing information describing bond interface characteristics. The disbonded region was easily discernible from the well-bonded region in the images. The images also show that the disbonded region looks quite different from that of the surrounding well-bonded region in sample F when the images obtained from the "bottom" of the specimen are compared with those obtained from the "top". The relatively "bright" disbond region observed when sample F was imaged from the "bottom" side and the "dark" disbond region observed when the sample was imaged from the "top" side agree with the corresponding echo decay patterns obtained with the contact transducer; i.e., a relatively higher attenuation associated with the disbonded region when interrogated from the "top" when compared with the results obtained from the "bottom". These results suggest that the images obtained with the linear array convey information regarding the characteristics of the interface between the aluminum and the disbond. Thus suggesting that medical linear array imaging technology may offer a useful means for developing a rapid, real-time, and portable method of adhesive bond inspection and characterization.